

AD-A100 594

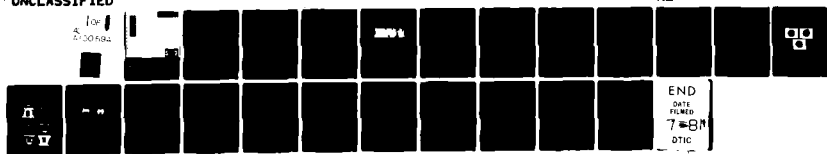
MCDONNELL DOUGLAS ASTRONAUTICS CO-ST LOUIS MO  
IMPROVED INJECTION LASER WAVEGUIDE COUPLER. (U)  
MAY 81 P BEAR

F/6 20/5

N00173-79-C-0470  
NL

UNCLASSIFIED

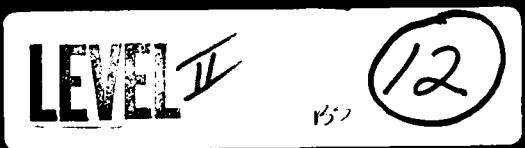
for  
200482



END  
DATE  
FILED  
7-8-81  
DTIC

DTIC FILE COPY

AD A100594



DTIC  
SELECTED  
JUN 25 1981  
S D

MCDONNELL DOUGLAS ASTRONAUTICS COMPANY-ST. LOUIS DIVISION

MCDONNELL DOUGLAS  
CORPORATION

DISTRIBUTION STATEMENT A

Approved for public release;  
Distribution Unlimited

81610123

Accession For	<input checked="" type="checkbox"/>	
NTIS GRA&I	<input type="checkbox"/>	<input type="checkbox"/>
DTIC TAB	<input type="checkbox"/>	<input type="checkbox"/>
Unannounced	<input type="checkbox"/>	
Justification		
By <u>Per Ltr. on file</u>		
Distribution/		
Availability Codes		
Avail on /or		
Dist	Special	
<u>A</u>		

COPY NO. \_\_\_\_\_

16 **IMPROVED INJECTION LASER**  
**WAVEGUIDE COUPLER.**

9 **FINAL REPORT.**

11 **MAY 1981**

12 23

10  
 Prepared by: Philip Bear

Prepared For: Naval Research Laboratory, Washington D.C. 20375  
13 Contract No. N000173-79-C-0470 CDRL Sequence No. A002

**MCDONNELL DOUGLAS ASTRONAUTICS COMPANY-ST. LOUIS DIVISION**

Box 516, Saint Louis, Missouri 63166 (314) 232-0232

**MCDONNELL DOUGLAS**  
  
 CORPORATION

403930

## 1.0 INTRODUCTION

This report summarizes the results of the Improved Injection Laser/Waveguide Coupler Program (contract N00173-79-C-0470) which follows initial development carried out on the Injection Laser/Waveguide Coupler Program (contract N00173-78-C-0087). The present program goal was to enhance the waveguide coupler design to provide a device which can be aligned with a standard micromanipulator and achieve 50% or better coupling efficiency. The design approach was to develop static mechanical spacers for the waveguide coupler which furnish easy and precise transverse and longitudinal positioning of a  $\text{LiNbO}_3$  waveguide with respect to an injection laser diode.

The program was to include the following tasks: (1) modify the waveguide coupler design and assembly procedures to provide a device that can be readily assembled and will achieve near theoretical coupling efficiency; (2) fabricate these optimized couplers using Hitachi laser diodes and evaluate these devices; (3) deliver two couplers without  $\text{Ti:LiNbO}_3$  waveguides attached; and (4) provide a cost estimate for the fabrication of ten such units.

This final report is being submitted as a deliverable item as required by the contract Statement of Work.

The study leader at MDAC-STL was Mr. Philip D. Bear, Electrooptics Department (E413). Other personnel at MDAC-STL who contributed significantly to the program included Dr. Robert Rice, design and technical discussions; Mr. John Powers, processing of silicon substrates; Mr. Herbert Koenig, laser diode bonding; Dr. Dennis Hall, coupling analysis; and Mr. Gordon Burkhardt, component polishing.

Since the improved waveguide coupler program was a continuation of an earlier contract, a review of the former program is appropriate. There were three significant achievements under that program. First, an analytical and experimental study was made on the mode profiles of titanium indiffused  $\text{LiNbO}_3$  waveguides. Second, a coupling study was performed in which laser to waveguide coupling efficiency was calculated and measured as a function of transverse, longitudinal, and angular displacement. Third, the polishing and coating (AR) of  $\text{LiNbO}_3$  waveguide material was developed to the point of being a routine procedure.

The waveguide coupler developed in the preceding program is presented in Figure 1. It consisted of an oxidized silicon substrate, injection laser

## WAVEGUIDE COUPLER DESIGN

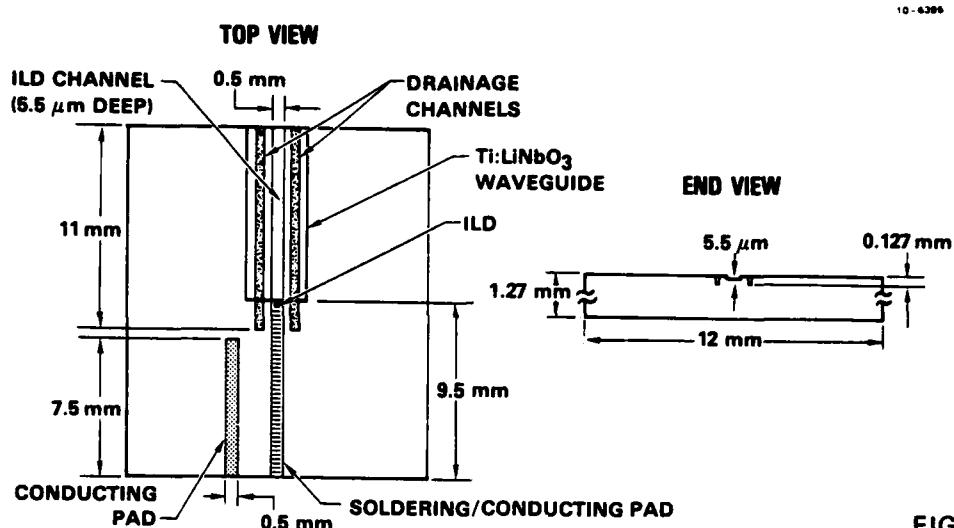


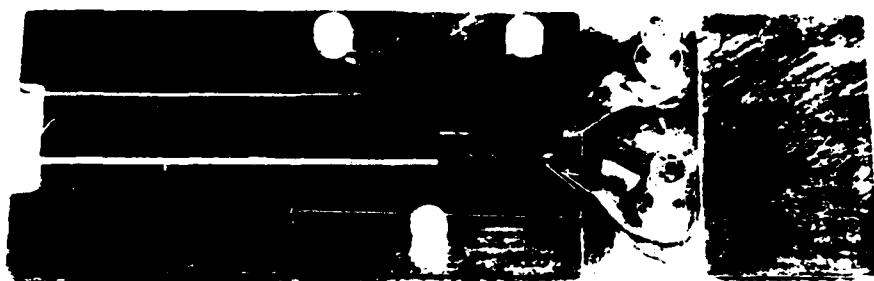
FIGURE 1

diode (ILD),  $\text{Ti:LiNbO}_3$  waveguide, conducting pads, and bond wires. The substrate had a 1 mm wide by 0.005 mm deep channel in which a 9.0 mm long by 0.5 mm wide conducting/soldering pad was deposited. The coupler required ten fabrication steps: (1) a 50.4mm x 1.27 mm thick silicon wafer was cut to the designed configuration, (2) two channels were chemically etched into the [100] silicon which served as deep drainage channels for the cement used for waveguide bonding, (3) another channel was chemically etched into the silicon which served to align the ILD junction to the plane of the waveguide, (4) a layer of silicon dioxide ( $\text{SiO}_2$ ) was thermally grown over the entire surface to provide electrical insulation and a relatively low refractive index interface between the waveguide and substrate, (5) the conducting pads were deposited, (6) indium was plated over the electrode in the channel, (7) the ILD was soldered at the edge of the indium pad, (8) wire leads were bonded from the ILD to the wider electrode, (9) the waveguide was actively aligned and coupled to the ILD, and (10) the waveguide was bonded onto the substrate.

The  $\text{LiNbO}_3$  waveguide was aligned with the laser diode by holding the waveguide on a series of stages which provided three translational and two rotational degrees of freedom. With these five degrees of freedom, the waveguide could

be maneuvered into position and cemented into place. Because of the tight alignment tolerance in the transverse dimension, the coupler chips achieved only a 5% - 10% throughput. Figure 2 shows a photograph of one of two coupler units which were delivered to NRL.

### PHOTOGRAPH OF THE WAVEGUIDE COUPLER



10-6401

FIGURE 2

## 2.0 TECHNICAL DISCUSSIONS

### 2.1 New Design for Coupler

To provide a laser/waveguide coupler which would provide 50% or better coupling efficiency as well as easy alignment the coupler chip design had to be modified. Gaussian beam coupling theory<sup>1-4</sup> has shown that maximum coupling occurs when a laser diode is butt-coupled to a waveguide with the laser mode centered on the waveguide mode. The most common reasons for reduced coupling are transverse and longitudinal misalignments. Figure 3 presents a comparison of peak theoretical and experimental coupling efficiency as a function of longitudinal separation. Since waveguide losses reduced the measured light below the theoretical level, the ordinate in Figure 3 shows optical throughput, and the abscissa shows the longitudinal separation (Z) between the laser and waveguide in units of micrometers. It was evident that the data closely fitted the curves generated for coupling to waveguides with waists near 1.4  $\mu\text{m}$  when the maxima of the curves were normalized to the data at  $Z = 0$ . It should also be noted that the throughput fell to half the maximum value at about  $Z = 15 \mu\text{m}$ .

To determine the coupling sensitivity to transverse offset between the laser and waveguide, the coupled light was measured as the laser was translated

## LONGITUDINAL SENSITIVITY THEORY AND EXPERIMENT

10-6306

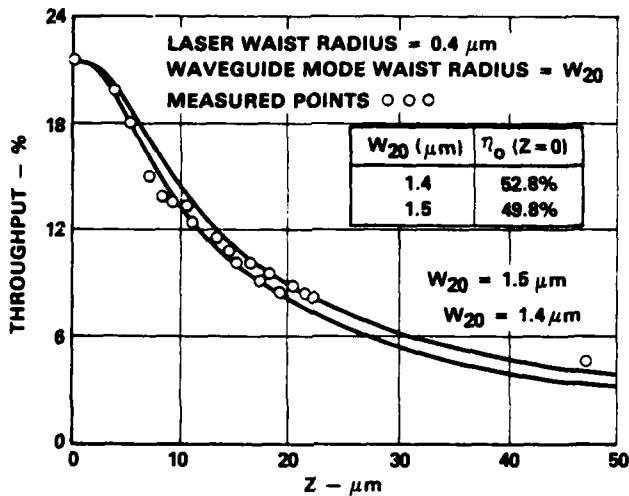


FIGURE 3

past the waveguide at a constant value of  $Z$ . The curve which was generated was Gaussian in shape and the full width at half the maximum intensity (FWHM) is shown in Figure 4 as a function of the longitudinal separation. At any abscissa value ( $Z$ ) one half of the FWHM gives the transverse offset which reduced the coupling to one half the peak value. Therefore, Figure 4 shows

## FWHM VS LONGITUDINAL SEPARATION

10-6302

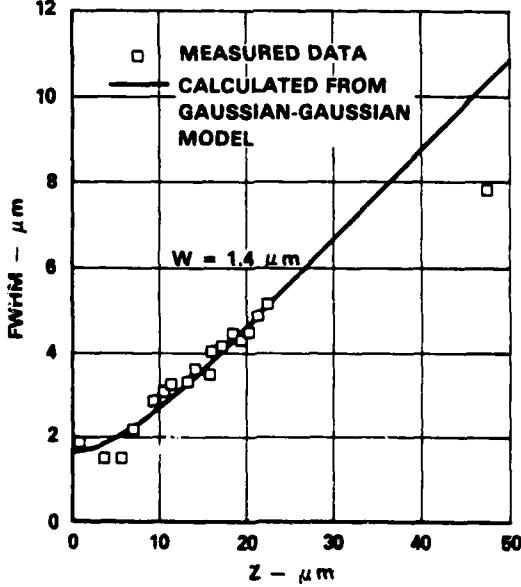


FIGURE 4

that for  $Z \leq 10 \mu\text{m}$  a transverse offset on the order of  $1.0 \mu\text{m}$  reduced the coupling by one half. It is clear that the transverse positioning was much more critical than the longitudinal.

The work described above provided the design tolerances for the transverse and longitudinal spacers to be used. Figure 5 illustrates the additions made to the original coupler design. The small circles which are labeled as spacer pads were Al pads which provided the transverse alignment. The horseshoe shaped piece

### LASER/WAVEGUIDE COUPLER

#### IMPROVED VERSION

10-6394

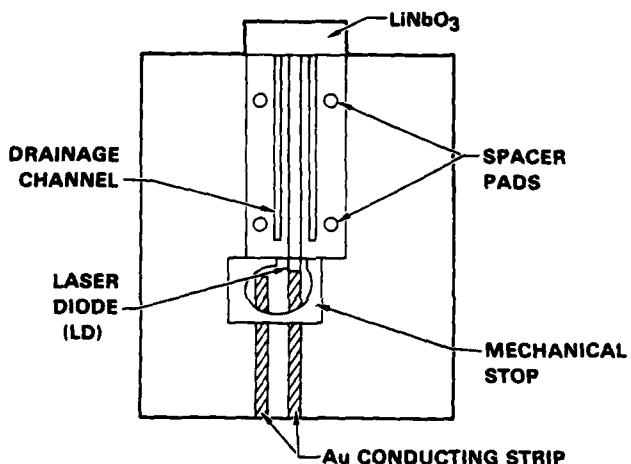


FIGURE 5

which is labeled "mechanical stop" provided the longitudinal alignment. Figure 5 shows a cross sectional view of the improved coupler made along the laser diode channel. On the left of the figure are the Au electrode stripe, solder, and the laser diode with the active region positioned at a height of  $d/2$  above the channel floor. The channel depth is shown as  $\ell$  and the mode waist in the waveguide is given as  $t$ . The height of the lasing region,  $d/2$ , was found by measuring the interference of the laser light and its reflection (Lloyd's mirror). The measured value was actually twice  $d/2$ , i.e., the spacing between the laser and its image. This will be discussed in more detail later. The channel depth  $\ell$  was determined with a Dektak profilometer while the guiding region thickness was obtained from coupling data as previously shown in Figure 3. These measurements allowed the spacer pad thickness  $T$  to be evaluated to  $0.1 \mu\text{m}$ . For a  $1.0 \mu\text{m}$  longitudinal separation a transverse error of  $0.3 \mu\text{m}$  changed the maximum

### MAGNIFIED SIDE VIEW CROSS SECTION OF LASER/WAVEGUIDE COUPLER

$$\text{SPACER PAD THICKNESS: } T = \frac{d}{2} - (l + \frac{t}{2})$$

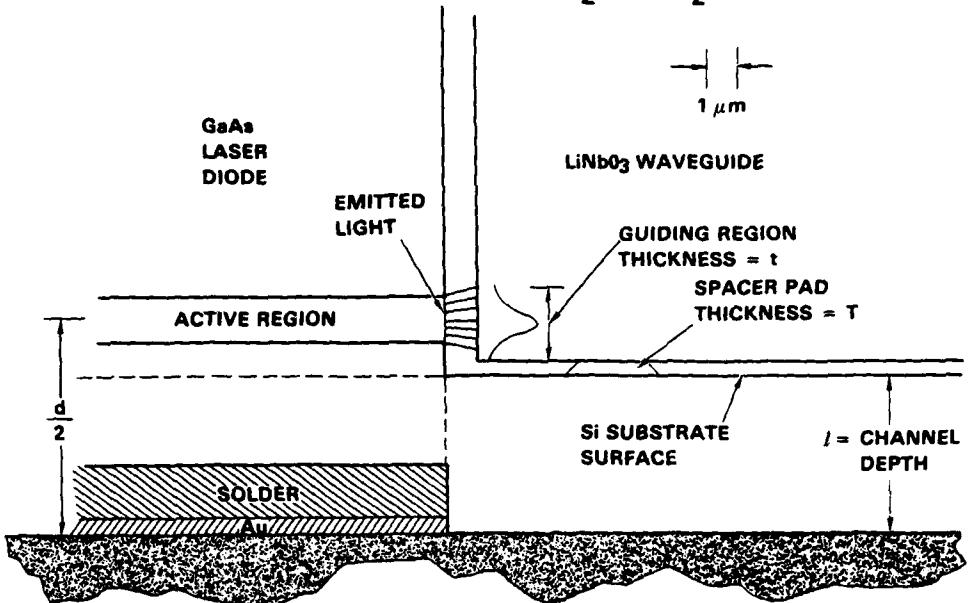


FIGURE 6

theoretical coupling from 83% to 77%. Therefore, error of this order did not produce an intolerable loss in coupling. When the required value for  $T$  had been determined, a mask was placed on the coupler and the four Al pads were deposited by thermal evaporation.

An enlarged view of the horseshoe shaped mechanical stop is shown in Figure 7a. It was made from stainless steel so that it was hard enough to be polished easily. The surfaces which contacted the coupler surface and the waveguide were polished flat and perpendicular. Another piece which is shown in Figure 7b was used to align the mechanical stop. This "pseudo waveguide" also had the bottom side and one end polished flat and perpendicular. On the polished end a metallic spacer was deposited as shown in Figure 7b. The top surface was given a thin metallic coating, and the lower edge, which was near the laser, was given a very slight bevel.

To align the mechanical stop the pseudo-waveguide was slid up to the laser so that the thick part of the metallic spacer was in contact with the laser. The beveled edge prevented the pseudo-waveguide from damaging the lasing region of the laser diode. The mechanical stop was then slid up to the pseudo-waveguide

## LONGITUDINAL SPACER FABRICATION COMPONENTS

10-6387

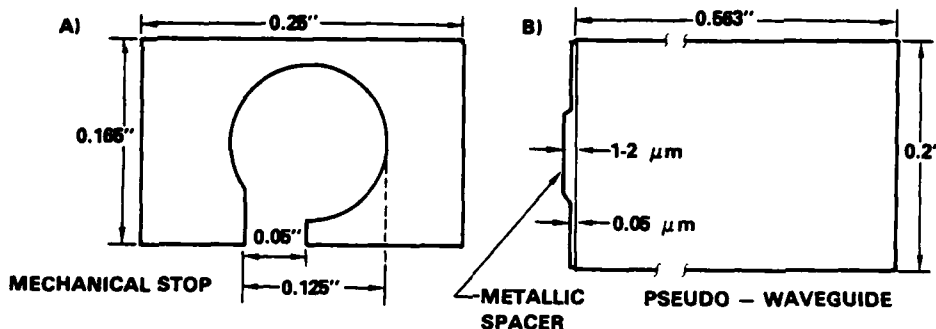


FIGURE 7

as shown in Figure 8. Contact was determined by looking for electrical continuity from the mechanical stop to the metal vacuum chuck which held the pseudo-waveguide. When this occurred the mechanical stop was cemented into place and the pseudo-waveguide was removed. The  $\text{LiNbO}_3$  waveguide was then slid up to the mechanical stop, which placed it about  $1 \mu\text{m}$  from the laser, without actually contacting the laser. The  $1 \mu\text{m}$  spacing protected the laser and waveguide without seriously reducing the coupling efficiency. Another change from the previous program involved the use of Hitachi HLP1000 series laser diodes. These diodes had a threshold of 55 - 60 mA and a beam waist of  $0.75 \mu\text{m}$ . This

## SKETCH OF ARRANGEMENT FOR SETTING THE LONGITUDINAL ALIGNMENT

10-6380

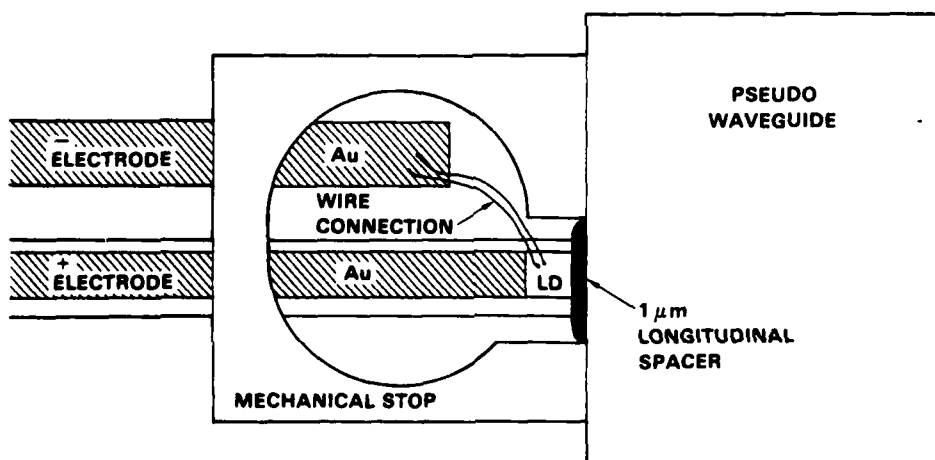


FIGURE 8

large waist provided a mode which matched the size of the waveguide mode rather well and, therefore, the theoretical maximum coupling was 83%.

## 2.2 Coupler Construction

The steps for fabrication of the Si coupler substrate were described in the Introduction. When a substrate was received from the Si processing laboratory, it lacked the laser diode and the spacers. Before the laser was bonded down, a thin layer of indium was electroplated onto the end of the positive Au electrode. Since the laser was wider than the Au band, two pieces of Au foil were placed on each side of the metallized region. The laser was then pushed down into the molten indium with the p-side down. The Au shims helped control the chip position so that the laser was not bonded either too low or too high. If the laser was too low, the waveguide could not be coupled even without the Al pads; whereas, if the laser was too high, it was difficult to evaporate sufficiently thick Al pads which adhered adequately.

Following the laser bonding, the coupler had two Al wires ultrasonically bonded between the n-side of the laser and the second Au electrode strip. At this point, the depth of the channel in the substrate was measured by the Dektak profilometer. This measurement was done after the Si processing was finished but before the Al pad deposition. The Lloyd's mirror experiment was then performed to determine the laser height. Once this was completed, the required pad thickness was calculated and the Al pads were thermally evaporated onto the coupler. After pad deposition, the mechanical stop was cemented into place. To do this the pseudo-waveguide was slid up to the diode, the stop was placed around the laser and in contact with the pseudo-waveguide, and the stop was cemented to the coupler. The coupler fabrication was complete at this point and the coupling efficiency measurement could begin.

## 2.3 Preparation of the Waveguide

The waveguides used for this study were residuals from the previous coupler program. The one chosen for coupling measurement was repolished on each end as well as AR coated for  $\lambda = 0.83 \mu\text{m}$ . To avoid the annoying substrate modes which occurred when alignment was not perfect, the  $\text{LiNbO}_3$  was roughened on the side opposite the waveguide. This rough side and most of the exit end of the  $\text{LiNbO}_3$  were then painted with a black ink. Most of the substrate light was absorbed when this procedure was followed.

#### 2.4 Coupling Efficiency Measurement

Determination of the coupling efficiency of the waveguide couplers was accomplished with an integrating sphere. To do this the coupler was inserted horizontally into the sphere with the laser laying approximately in the plane of the hole in the sphere. The hole was on the equator and the detector looked down through the north pole. The coupler could be inverted without changing the detector output, which indicated that the highly diverging laser beam was making at least one reflection from the sphere wall before becoming incident upon the detector. Following this measurement the waveguide was slipped into place on the coupler and another measurement was made. The ratio of these two values gave the fraction throughput. In order to obtain the coupling efficiency the waveguide must be analyzed for scattering losses.

The scattering losses were found by using an Hitachi Laser diode mounted in a McDonnell Douglas double-sided heat sink and end-fire coupling the laser into the waveguide. The guided light was allowed to propagate through the waveguide and exit the opposite end. The goal was to find a maximum for the ratio of the guided light to the light emitted by the laser. The maximum obtained was 55%. When this was attained and the guided light was viewed on a screen, it was very bright and no substrate modes were visible. This ratio can be written as

$$\frac{P_{WG}}{P_{LD}} = \rho n$$

where  $P_{WG}$  and  $P_{LD}$  are the power of the waveguide light and the laser diode light respectively. The coupling coefficient is  $n$  and  $\rho$  represents the transmission through the waveguide, which includes the effects of the losses due to waveguide scattering. Assuming that near theoretical coupling was achieved when 55% throughput was reached, the value of  $\rho$  was 0.66. This represents a waveguide loss of 1.8 dB/cm which was not unreasonable. If  $P_{WG}/P_{LD}$  was 0.33 or greater, the coupling efficiency was at least 50%.

#### 2.5 Substrate Flatness Measurement

After several efforts to produce a waveguide coupler with high coupling efficiency, it was determined that the Si material from which the substrates were made was not sufficiently flat. The material was n type Si which was two inches in diameter

by 0.050 inches thick and was grown at Monsanto by the Czochralski method in the [100] orientation. Figure 9 presents interferograms of three of these Si wafers in which the change in elevation between interference minima is 0.3164  $\mu\text{m}$ . Although these surfaces were topographically interesting, they were not sufficiently flat to allow waveguide alignment to within tenths of a micrometer. Subsequent to this discovery the substrates were polished.

### INTERFEROGRAMS OF THREE SI WAFERS

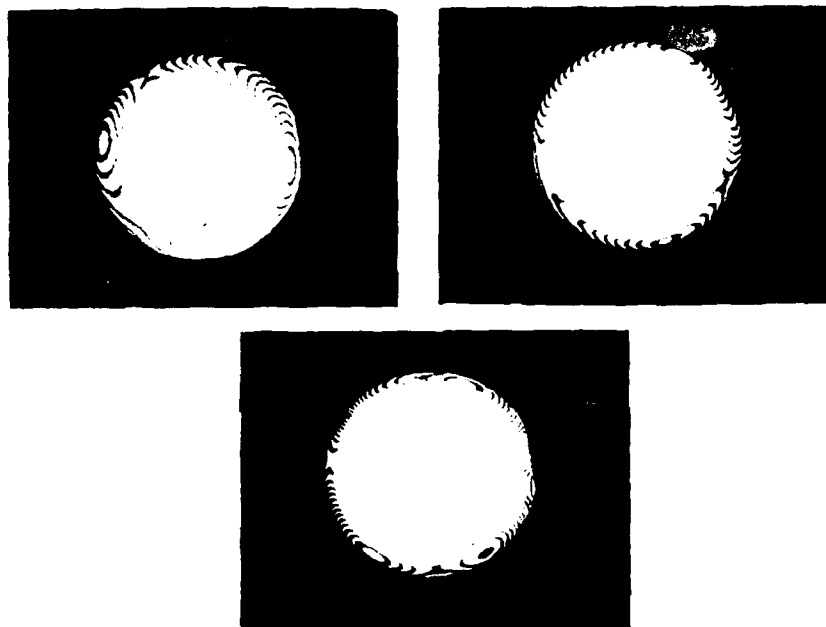


FIGURE 9

The photographs shown in Figures 10 and 11 were taken of waveguide coupler substrates as viewed on a Carl Zeiss flatness tester. The shorter ends of the substrates were supported by microscope slides and, therefore, the interference produced by these slides should be ignored. The wavelength used for these photos was the 0.546  $\mu\text{m}$  Hg line so that the distance between interference minima is 0.273  $\mu\text{m}$ . The surfaces as seen in Figure 10a and 11a were unpolished. The substrate in Figure 10a was a finished substrate with etched channels and gold electrodes, whereas the Si wafer shown in Figure 11a had no processing other than cutting to shape. Figures 10b and 11b show the substrate surfaces after polishing but before any coupler fabrication processing was begun. Figure 10b shows the drainage channels because they were too deep to be polished away. Figures 10c, d and 11c, d illustrate that the Si substrate processing can be completed without damaging the surface figure.

### FLATNESS MEASUREMENT OF SUBSTRATE TWO

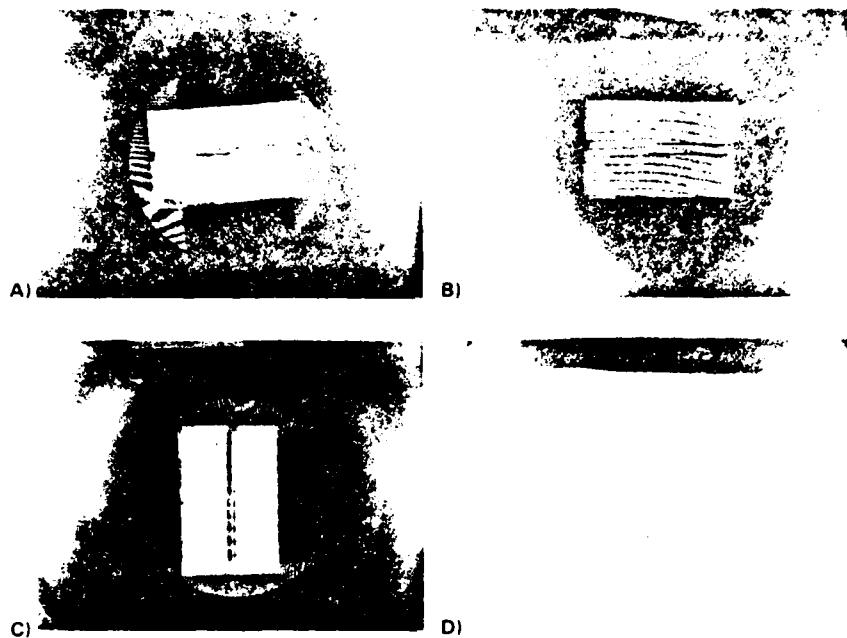


FIGURE 10

### FLATNESS MEASUREMENT OF SUBSTRATE ONE

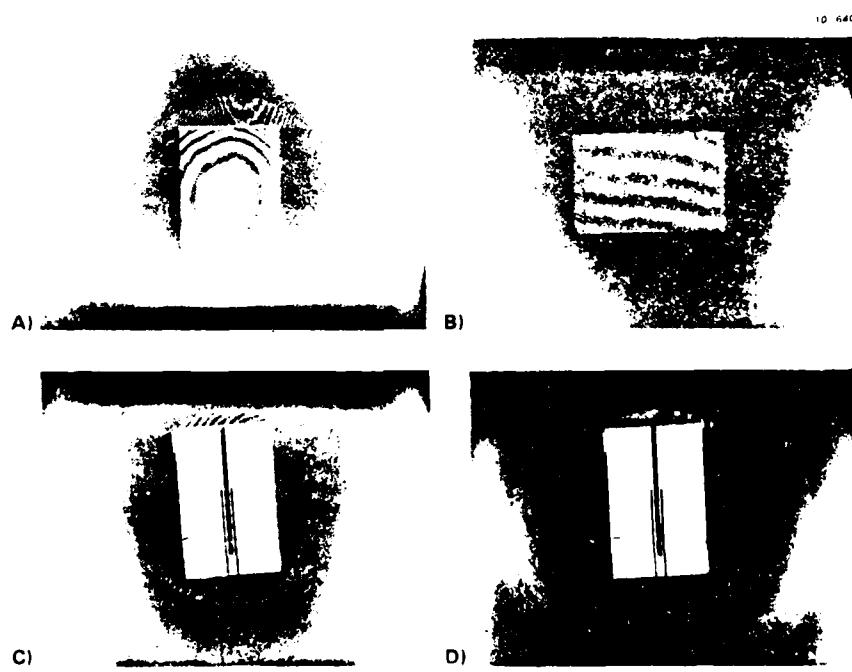


FIGURE 11

In addition to the Si substrates, the  $\text{LiNbO}_3$  waveguides were measured for surface flatness. Two typical waveguides are shown in Figure 12. The waveguides were polished prior to the Ti indiffusion but this occurred during the previous waveguide coupler program; therefore, no pictures of the waveguide flatness were taken prior to indiffusion.

### FLATNESS MEASUREMENT OF $\text{LiNbO}_3$ WAVEGUIDES

10-6397

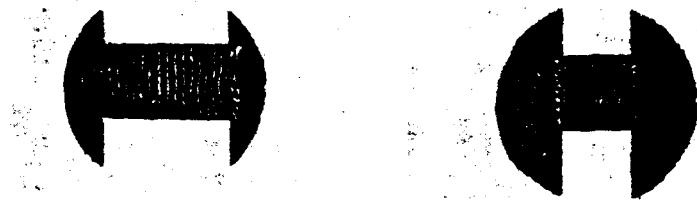


FIGURE 12

#### 2.6 Problems Encountered

Since several of the problems encountered were centered around the laser diode bond, the resolution of these will be discussed first. Although the strength of the laser bond was typically not a problem, when the bond was weak this was discovered during the wire bonding, at which time the laser diode detached from the substrate. Therefore, the wire bonding acted as a quality control procedure for laser diode bond strength.

It was found that the height of the laser diode varied from bond to bond due to varying indium thickness. This variation in the laser height directly affected the required thickness for the Al spacer pads on which the waveguide rested. If the spacer pads were thicker than  $1-1 \frac{1}{2} \mu\text{m}$  the adhesion of the pads was poor; therefore, the laser bond thickness needed to be controlled. This was accomplished by placing thin Au leaf under each side of the laser to act as shims, so that when the laser was pushed down into the molten indium it stopped within an acceptable range of heights. This allowed reasonable thicknesses for thermal evaporation of the spacer pads.

During the course of this program the laser diode bonding technique was being examined due to diffusion problems which are inherent to indium bonding. For

several substrates the bonding was done to a very thin (500 Å) Au electrode strip. It was found that the resistance of these strips was too high and the strips acted as heaters when current passed through them. When the Au electrodes were 0.5  $\mu$ m thick the resistance was low and the bonding was good.

During the coupling measurements it was found that unwanted light was entering the detector along with the coupled light. Since the waveguide coupler never achieved the maximum theoretical coupling it is clear that the laser to waveguide alignment was not perfect. When this occurred light from the laser traveled down the channel which was under the waveguide and combined (in the viewing plane) with the guided light which was exiting the waveguide. If this light intensity were measured and used to calculate the coupling efficiency the result would be too large. If any future substrates are made by terminating the etched channel before reaching the edge of the Si substrate, the problem can be reduced, if not eliminated. This would reduce the area of the light path by  $\gtrsim 80\%$  for the light which is interfering with the measurement.

## 2.7 Analytical Work

### 2.7.1 Waveguide Modes

The problem of coupling a Ti:LiNbO<sub>3</sub> waveguide to a GaAlAs double-heterostructure laser diode has been well studied<sup>2,3,4</sup>. As demonstrated on the earlier coupling program, the coupling efficiency was far more sensitive to transverse misalignment than to longitudinal misalignment. The edge-coupling process could be described quite accurately by a Gaussian coupling model<sup>3</sup>, and some of this work was reported in the previous Final Report (N00173-78-C-0087). Since that time even more confidence has been gained in the application of this model to the laser-to-waveguide coupling problem. Figure 3 showed a plot comparing the measured and calculated "throughput" (edge-coupled) in and prism coupled out) as a function of longitudinal separation Z. Since both a laser waist and a waveguide waist parameter were needed to compare the experiment to the calculation, the laser waist was obtained independently by measuring the laser's far-field pattern, and the waveguide parameter was treated as a fitting parameter. The consistency of the Gaussian coupling model for this application was tested by comparing the theoretical and measured m-line intensity as a function of the transverse alignment parameter  $\Delta$ . Figure 4 shows a comparison of a full-width at half-maximum

(FWHM) of the coupling curves as a function of  $Z$  obtained from both theory and experiment. Good agreement was found between the experimental results and the predictions of the model using the same parameters obtained for the fit shown in Figure 3. The model was thus both internally consistent and reliable.

The data presented in Figure 4 showed that for  $Z = 0$ , a transverse misalignment of roughly  $0.75 \mu\text{m}$  in either direction reduced the coupled power to 50% of its maximum value. To assist in placing the laser junction with respect to the larger waveguiding layer, the fitting procedure for the coupling data was used to estimate the depth below the waveguide surface of the maximum waveguide mode intensity. The goal was to center the laser junction about that position on the waveguide edge. To make the estimate, the model for the waveguide mode given by the equations

$$\psi_2(x) = BX \exp [-(x/W_2)^2], \quad x \geq 0 \quad (1)$$

and

$$\psi_2(x) = 0, \quad x < 0 \quad (2)$$

where  $\psi_2(x)$  is the electric field of the waveguide mode,  $B$  is a constant,  $W_2$  is a width parameter, and  $x = 0$  defines the air/waveguide interface. This model was studied in an earlier work<sup>4</sup> and was found to provide a good description of the actual asymmetric waveguide mode. Figure 13 presents

### COMPARISON OF MODE PROFILES

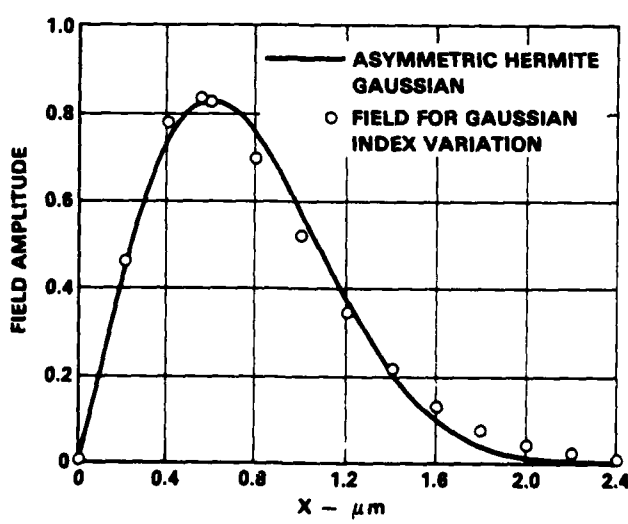


FIGURE 13

a comparison of Eq. (1) with Hocker's numerical results<sup>5</sup> for an assumed Gaussian refractive index profile and waveguide parameters<sup>6</sup>  $b = 0.410$  and  $V = 4.30$ . The position of the maximum of  $\psi_2(X)$  was located at  $X_{\max} = W_2/\sqrt{2}$ , and so  $W_2$  was extracted from a waveguide measurement then  $X_{\max}$  was easily determined.

While  $W_2$  was a parameter necessary for the evaluation of  $\psi_2(X)$ , it was not the 1/e half-width of  $\psi_2(X)$ . The values of  $X$  for which  $\psi_2(X)$  equals 1/e of its maximum satisfied the equation:

$$(X/W_2) \exp [-(X/W_2)^2] = (\sqrt{2})^{-1} \exp (-3/2) \quad (3)$$

By graphically solving Eq. (3) and defining  $W$  to be the 1/e half-width of  $\psi_2(X)$ , it was shown that;

$$W \approx 2 W_2/3 \quad (4)$$

Therefore, if, for a given waveguide, a procedure such as that which led to Figures 3 and 4 determined a value of  $W$  for that waveguide, the position of maximum mode intensity was;

$$X_{\max} = \frac{1}{\sqrt{2}} - \frac{3}{2} W = 1.06 W \quad (5)$$

Interestingly enough, had it been assumed that the waveguide mode were a symmetric Gaussian with a 1/e point located at  $X = 0$ ,  $X_{\max} = W$ .

The second technique for determining an approximate value for  $W$ , and hence  $X_{\max}$ , was to measure the radiation coupled out through the waveguide edge, assume it propagated as a Gaussian, measure its far-field divergence angle, and infer a Gaussian waist size in the usual way. In Figures 14 and 15 plots are shown of  $X_{\max}/\lambda$  as a function of the angle between the optic axis and the half-power point of the radiation pattern. The functional relationship was;

$$X_{\max}/\lambda = \alpha/\tan \theta_{1/2} \quad (6)$$

where  $\alpha = 0.199$  for the electric field of Eq. (1) and  $\alpha = 0.188$  for an assumed symmetric Gaussian form.

### DEPTH OF MAXIMUM MODE INTENSITY

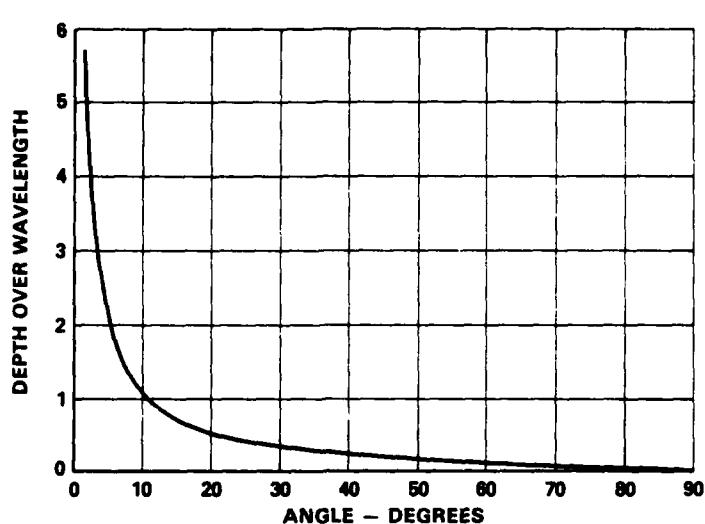


FIGURE 14

### DEPTH OF MAXIMUM MODE INTENSITY

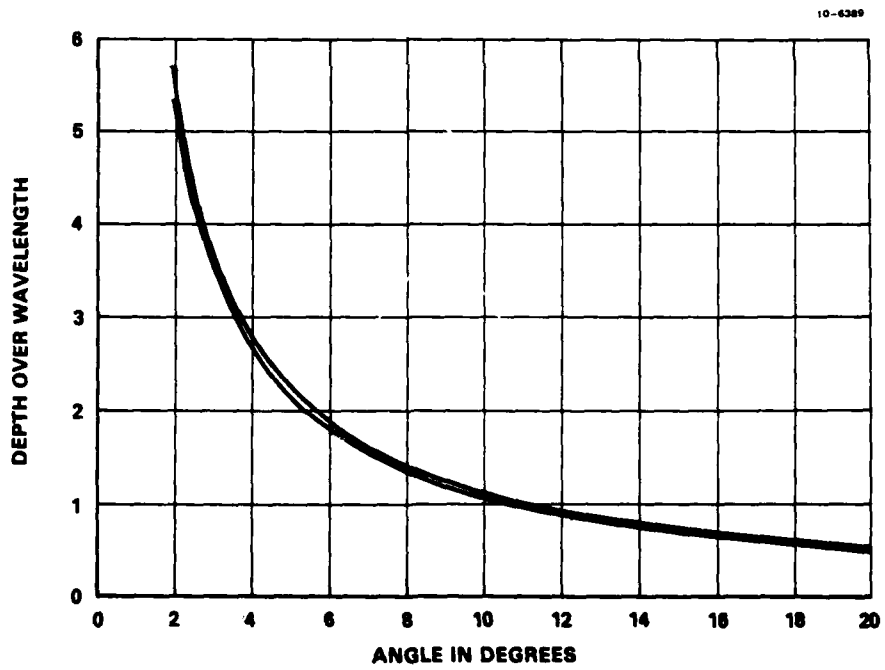


FIGURE 15

#### 2.7.2 Lloyd's Mirror Analysis

An analysis of the Lloyd's mirror experiment using Gaussian beams was done to determine the validity of using the simple equation

$$\frac{d}{2} = \frac{\lambda D}{2y} \quad (7)$$

where  $d/2$  is the height of the laser from the surface,  $\lambda$  is the wavelength,  $D$  is the laser to observation plane distance, and  $X$  is the length in the observation plane between the extrema of the interference pattern. Figure 16 illustrates the geometry of Lloyd's mirror experiment.

### LLOYD'S MIRROR EXPERIMENT

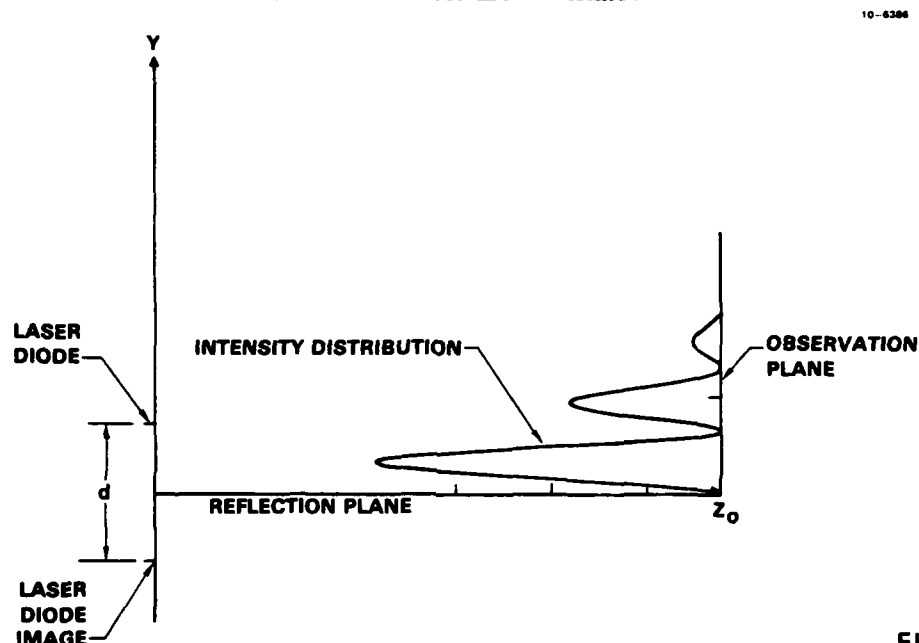


FIGURE 16

The electric field of a laser diode is elliptical and can be written as<sup>7</sup>

$$E(x, y, z) = E_0(z) \exp \left\{ -x^2 \left[ \frac{1}{w_x^2(z)} + \frac{ik}{2R_x(z)} \right] - y^2 \left[ \frac{1}{w_y^2(z)} + \frac{ik}{2R_y(z)} \right] \right\} \quad (8)$$

where  $E_0(z)$  is a  $z$ -dependent amplitude which was constant for this analysis,  $w_x$  and  $w_y$  are beam radii for the  $x$  and  $y$  directions,  $R_x$  and  $R_y$  are the field radii of curvature for the  $x$  and  $y$  directions, and  $k$  is  $\frac{2\pi}{\lambda}$ . Equation (8) can be rewritten for the source at  $y = d/2$  and observation in the  $x = 0$  plane as

$$E_1(0, y, z_0) = E_0(z_0) \exp \left\{ - \left( y - \frac{d}{2} \right)^2 \left( \frac{1}{w_y^2(z_0)} + \frac{ik}{2R_y(z_0)} \right) \right\}, \quad (9)$$

and the image at  $y = -d/2$  can be written as

$$E_2(0, y, z_0) = E_0(z_0) \exp \left\{ -\left(y + \frac{d}{2}\right)^2 \left( \frac{1}{w_y^2(z_0)} + \frac{ik}{2R_y(z_0)} \right) - i\pi \right\}. \quad (10)$$

The  $\exp(-i\pi)$  in equation (1) produces the phase change which occurs upon reflection from the silicon substrate. Upon setting  $E_0(z_0) = 1$ , adding  $E_1$  and  $E_2$ , and squaring this sum, the field intensity can be written as

$$|E_T|^2 = \exp \left\{ -\frac{2\left(y - \frac{d}{2}\right)^2}{w_y^2} \right\} + \exp \left\{ -\frac{2\left(y + \frac{d}{2}\right)^2}{w_y^2} \right\} - 2 \exp \left\{ -\frac{2\left(y^2 + \left(\frac{d}{2}\right)^2\right)}{w_y^2} \right\} \cos \left( \frac{kdy}{R_y} \right). \quad (11)$$

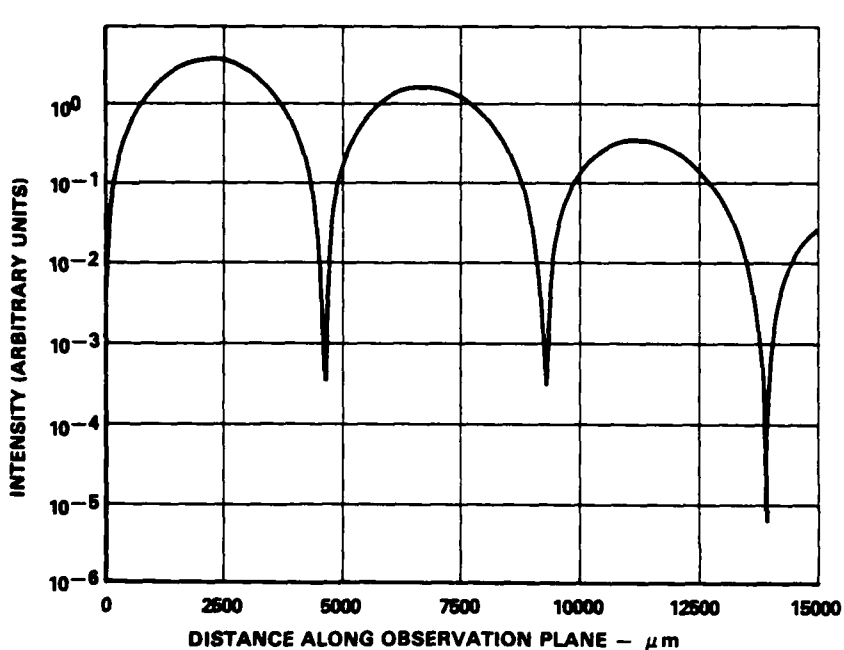
The equation was plotted in Figure 17 and showed the interference distribution. The abscissa shows the distance along the observation plane in micrometers which is  $y$  in Eq. (8). The calculation was done for  $d/2 = 8.25 \mu\text{m}$ ,  $\lambda = 0.83 \mu\text{m}$ , and  $z_0 = 9.2 \times 10^4 \mu\text{m}$ . The values of  $w_y$  and  $R_y$  were calculated<sup>7</sup> using the laser waist of  $0.75 \mu\text{m}$ .

A comparison of the calculated separation of the minima at  $y = 9272 \mu\text{m}$  and  $y = 4636 \mu\text{m}$  from Figure 17 and the first two minima of a Lloyd's mirror measurement showed agreement to 0.5%, while comparison of the calculation and data for the first two maxima shows agreement to within 2%. This indicated that the theoretical model accurately represents the experiment. Having established the model, it was found that the use of Eq. (7) was satisfactory when  $y$  represented the spacing between the first two minima, but when the first two maxima were used, a 4% error was introduced.

## 2.8 Alternate Design Approach

A design was developed which was to avoid some of the problems encountered with the baseline design. A side view of this second approach is shown in Figure 18. The basic waveguide coupler substrate (labeled Si) was cut in half and a laser diode was bonded onto the gold strip with its front facet extending slightly beyond the edge of the Si. This Si section was epoxy bonded to a baseplate. The second half of the Si which had the drainage channels was then clamped and bonded

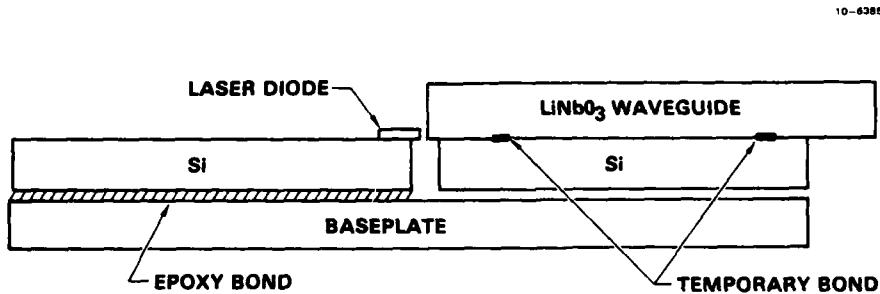
### LLOYD'S MIRROR INTERFERENCE DISTRIBUTION



10-6384

FIGURE 17

### ALTERNATE APPROACH TO THE WAVEGUIDE COUPLER



10-6385

FIGURE 18

temporarily to a waveguide. This Si/waveguide section was carefully maneuvered so that the laser diode coupled efficiently into the waveguide, which was determined by viewing the light emitted from the output waveguide edge. The Si was then bonded permanently to the baseplate and the temporary bond to the waveguide was to be broken. Upon replacing the waveguide on the Si and sliding it up to the laser, the light then should have coupled efficiently into the waveguide.

This technique was tried twice but both attempts reached an impasse during the final stages. The first problem was that after the temporary bond was dissolved the waveguide did not return to position and couple light effectively. In dissolving the temporary bond, the Si to baseplate bond was possibly affected and the correct spacing of the Si with respect to the laser diode subsequently lost. During the second attempt the proper positioning of the Si/waveguide section was lost after the cement was applied but before it was hardened. Re-positioning proved to be impossible since this required pushing the cement out from under the waveguide or sucking it back under the waveguide.

#### 2.9 Conclusions and Recommendations

The variation in tolerances of the components and the capability of present state-of-the-art micropositioning devices to obtain and hold mechanical position accuracies required for the laser diode to waveguide coupler are not adequate to obtain reliable devices that meet the program goal of 50% coupling efficiency. The positional stability of bonding materials for the laser diode and waveguide were also determined to be inadequate to maintain the precise tolerance required.

It is recommended that consideration be given to an R&D program to investigate the viability of a monolithic integrated optic approach for the laser diode to waveguide coupler using a common substrate.

Present state-of-the-art in mechanical positioning accuracy and long term stability to obtain the required accuracies do not warrant further investigation of this approach at the present time.

#### 2.10 Cost Estimate

Since there was no repeatable and practical mechanical positioning approach obtained during this program that achieved the program goal of >50% coupling efficiency, it is not possible to provide a cost estimate for ten coupler units.

REFERENCES

1. H. Kogelnik, in "Proceedings, Symposium on Quasi-Optics", J. Fox, Ed. (Polytechnic Press, Brooklyn, N.Y., 1964), p. 333.
2. W. K. Burns and G. B. Hocker, *Appl. Opt.* 16, 2048 (1977).
3. D. G. Hall, R. R. Rice, and J. D. Zino, *Opt. Lett.* 4, 292 (1979).
4. D. G. Hall, *Appl. Opt.* 18, 3372 (1979).
5. G. B. Hocker, Honeywell Corporate Research Center, "Diffused Optical Waveguide Modes," unpublished.
6. G. B. Hocker and W. K. Burns, *IEEE J. Quantum Electron.* QE-11, 270 (1975).
7. A. Yariv, "Quantum Electronics" (Wiley, New York, 1975), pp. 109-124.